EXTENDED OPTIMAL FILTERS FOR ADAPTIVE-ON-TRANSMIT RADAR SYSTEMS USING BINARY CODES

A. V. Alejos[1, 2, *], M. Dawood[2], and M. G. Sanchez[1]

[1]University of Vigo, Department Signal and Communications Theory, Maxwell St., Vigo E36310, Spain

[2]Klipsch School of Electrical and Computer Engineering, New Mexico State University, Las Cruces, NM 88003, USA

Abstract—This study introduces an extended optimal filtering technique for adaptive-on-transmit radar based on the transmission of pseudorandom noise waveforms as a method to simultaneously achieve low sidelobe level and spectral purity without degrading the main peak of the cross-correlation function. The proposed method is an extended version of the classical optimal filtering technique, resulting in longer codes with three simultaneously improved features that usually work in trade-off: 1) the cross-correlation function (CCF) sidelobe level is reduced in direct proportion to the filter length, K; 2) the out-of-band spectral suppression is at least 40 dB for pseudorandom binary sequences (PRBS); and 3) the frequency spectrum tail presents a decay given by K^{-4}, offering larger out-of-band frequency suppression. The proposed technique provides skew-symmetry to the input signal and is tested on PRBS, Barker, and Golay pair of complementary codes. The proposed codes are also demonstrated to be Doppler resistant and offer better multipath capability.

1. INTRODUCTION

The search for new codes with a given performance metrics is a common practice for many applications including radar applications. Often in this process, the objective is to improve upon a specific feature of the code. For example, a CCF with lower sidelobe levels can be achieved using codes with comparatively larger lengths. In order to obtain higher lengths some properties of well-known codes, such as the

skew symmetry [1], can be explored to reduce the search effort. An alternative choice would consist of designing a completely new code instead of making use of the property of an existing code. However, this option can lead to a larger research effort, sometimes required of introducing deep changes in the involved hardware structures. In this paper, we discuss a way to provide a skew-symmetry to a binary code of any length. This solution can be combined with a transmitter able to modify the transmitting signal, becoming the set in a powerful adaptive transmitter system.

In radar applications, adaptive-on-transmit (AT) techniques are used at the transmitting end as a way to combat the adverse effects of the dynamically changing propagation environment. One of these AT techniques consists of manipulating one initial waveform, usually binary coded sequences, to achieve a new transmitted sequence having some desired characteristics. Two of the desired characteristics are that: (1) the sidelobe level (SLL) of the cross-correlation between the transmitted and the received waveform is minimal, and (2) the spectrum of the transmitted sequence should be either fully band-limited and/or provide sufficient out-of-band suppression (OBS). This latter parameter is measured as the amplitude of the first sidelobe present in the frequency spectrum magnitude of the transmitted code. It is desirable to maintain an OBS value as low as possible.

A typical AT technique is given in the form of a waveform-filter pair [2, 3], as in Fig. 1. According to this technique, an input digital binary code s_M is transformed into a new code q_K via a matrix transformation A. This matrix acts on some aimed features of the original code s_M, such as the SLL noise, so the performance of this method can be seen as a filter. The resulting output q_K, termed reference code in [2, 3] is a new code having the same length as the filter $K > M$.

However, AT techniques can work only on one feature of the transmitted waveform, and as a result other attributes can be negatively impacted. This is also the case for the waveform-filter pair
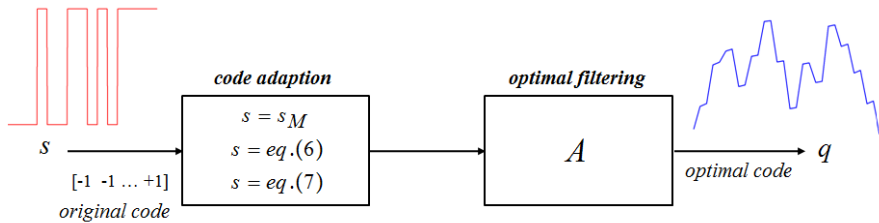

Figure 1. Functional diagram of waveform-filter pair.

method. If this technique is applied to a binary sequence, specifically, the pseudorandom binary sequence (PRBS) to reduce the SLL below a certain threshold, the OBS is negatively impacted. That is, the spectral purity of the transmitted signal will be compromised due to work in trade-off with the SLL.

In this paper, we report an improved method to obtain a waveform-filter pair suitable as an AT approach. This method makes use of skew-symmetry property such that better performing codes are obtained from an input binary code of any length. The outcome is a longer transmitted code, herein named as extended optimal code, which can achieve simultaneously both lower aperiodic CCF SLL, and spectrally clean waveforms with an increased OBS level, which becomes a positive feature, directly proportional to the filter/code length $K' \geq 2 \cdot M$. The main CCF peak, however, remains unaffected, and thereby enhances the dynamic range of the system as well as its ability to detect weaker returns. The outcome is a sidelobe spread-out measured in terms of integrated sidelobe level (ISL); the secondary sidelobes energy is distributed over a larger delay range. As a result, we find more samples of the CCF delay range with secondary sidelobes presence but with an amplitude level considerably reduced. The proposed extended technique indicates Doppler tolerance, and so an opposite tendency for the waveforms designed to achieve minimum CCF SLL.

The waveform-filter method presented herein has its roots in the classical optimal filter method [2, 3] which takes an input a binary code to transform it in an outcoming signal with reduced SSL. However, we demonstrate that this transformation only works properly with skew-symmetrical codes. Even for this case, the filtering proposed does not achieve an optimal performance in terms of equal distribution of secondary sidelobes energy or CCF ISL, nor an optimal frequency spectrum.

We show in Subsection 2.1 that this classical version presents an unbalanced distribution of the CCF SLL peaks. This fact was observed for the cases of PRBS and complementary codes [4], particularly with the Golay code pairs. Even though a modification to the classical optimal filter method is introduced to solve this limitation, the aimed trade-off between CCF SLL and OBS is not achieved. As a novel solution, we designed an extended version that achieves simultaneous improvement on both attributes for any kind of binary coded sequences. Subsequently, we refer our proposed method as the "extended version". Additionally, keeping the terminology used by Greip in [2], we apply the label "optimal" to indicate the finest simultaneous performance in terms of CCF SSL reduction, equal CCF ISL distribution and reduced OBS in the frequency spectrum.

Extended codes, as proposed here, possess narrowband features in the related frequency spectrum. This property impacts other important features, such as low probability of detection and intercept (LPD/LPI), immunity to external electromagnetic interference (EMI), spectral efficiency, and immunity to jamming.

In Section 2, we briefly discuss theoretical preliminaries related to classical optimal filters and their modified form. In Section 3, the extended version is discussed. This section highlights the commonalities and differences with the classical version. The performance analysis for Barker, PRBS and Golay codes is presented in Subsections 3.1, 3.2 and 3.3, respectively. This performance is compared to the given by other windowing techniques in Subsection 3.4. It is demonstrated in Section 4, that the proposed extended technique is Doppler resistant. Section 4 also discusses the multipath capabilities of the proposed extended codes. In Section 5, we briefly discuss the theoretical background, regarding concepts about the use of AT techniques, noise level mitigation as well as interest of the waveform-filter pairs. An overall scope about the possible application of the extended codes is also depicted in Section 5. Finally, conclusions are offered in Section 6.

2. BRIEF THEORETICAL BACKGROUND TO CLASSICAL OPTIMAL AND MODIFIED OPTIMAL FILTERS

2.1. Classical Optimal Filters

The optimal filtering technique [2, 3] can be applied to find an optimal code $q = \{q_K\}$ for a transmitted binary signal, $s = \{s_M\}$. The target feature is that the cross-correlation between the original and the new code offers minimal CCF SLL. This technique works well with codes having some symmetrical or repetitive behaviour, such as the Barker codes. However, it results in increased CCF SLL levels for codes with non-repetitive behaviour in the CCF shape and/or in the binary pattern, such as PRBS and/or Golay complementary code pairs, this latter with skew-symmetrical pattern [5]. A skew-symmetric binary sequence is formed by interleaving an odd length symmetric sequence with an even length asymmetric sequence. This means that a skew-symmetric binary sequence $(a_0, a_1, \ldots, a_N)$ meets the condition $[(a_j \cdot a_{j+k}) + (a_{N+1-j-k} \cdot a_{N+1-j}) = 0]$, for odd k, implying that all even length autocorrelation sums are 0. All odd-length Barker sequences are skew-symmetrical. Skew-symmetrical sequences are known to attain the optimal merit factor value [6–8].

As an example, we compare in Fig. 2, the ideal auto-correlation function (ACF) corresponding to the $M = 13$ bit Barker code

together with the CCF achieved using the classical optimal filtering technique [2, 3]. For the latter, we generated an optimal code $q_{K,M}$, with length $K = 2 \cdot M + 1 = 27$. The original Barker code used in this example was $s_{13} = \{-1, -1, -1, -1, -1, 1, 1, -1, -1, 1, -1, 1, -1\}$ and the new code obtained with the classical filtering technique $q_{27,13}$ is indicated in Appendix A.

In Fig. 3 we show the spectrum $S(f)$ corresponding to both codes, s_{13} and $q_{27,13}$. In Fig. 2, the resulting CCF for $q_{27,13}$ offers an improvement of $0.6\,\mathrm{dB}$ in ISL compared to the ACF of the original Barker code s_{13}. However, OBS using classical filtering technique worsens, as shown in Fig. 3.

If the same classical optimal filtering technique is applied to the $M = 15$ PRBS $s_{15} = \{-1, -1, -1, 1, -1, -1, 1, 1, -1, 1, -1, 1, 1, 1, 1\}$, a slight improvement of $1\,\mathrm{dB}$ is seen in the ISL level, while the OBS increases by $1\,\mathrm{dB}$. The classical filtering technique also resulted in a non-symmetric CCF, as shown in Fig. 4. The magnitude of the frequency spectrum $S(f)$ corresponding to both s_{15} and $q_{31,15}$ is plotted in Fig. 5.

In a similar manner, we have obtained Fig. 6 and Fig. 7, for the pair of Golay complementary sequences $sa_{16} = \{1, 1, 1, -1, 1, 1, -1, 1, 1, 1, 1, -1, -1, -1, 1, -1\}$ and $sb_{16} = \{1, 1, 1, -1, 1, 1, -1, 1, -1, -1, -1, 1,$
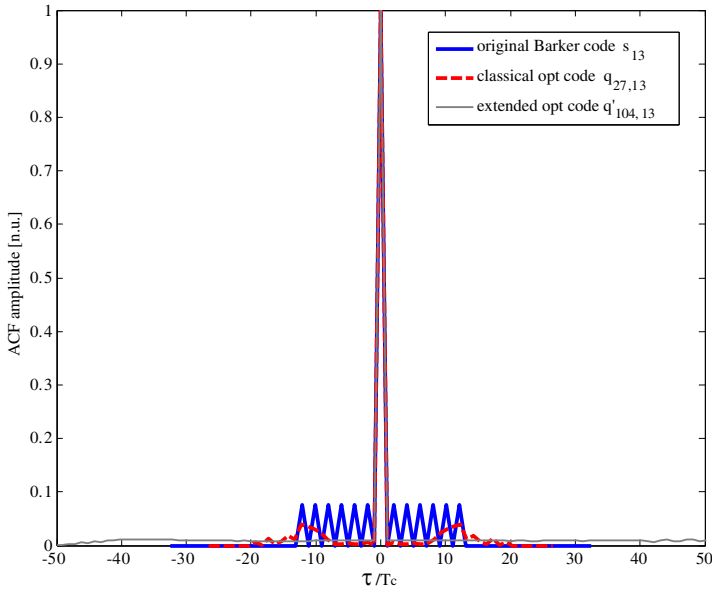

Figure 2. ACF corresponding to Barker case.
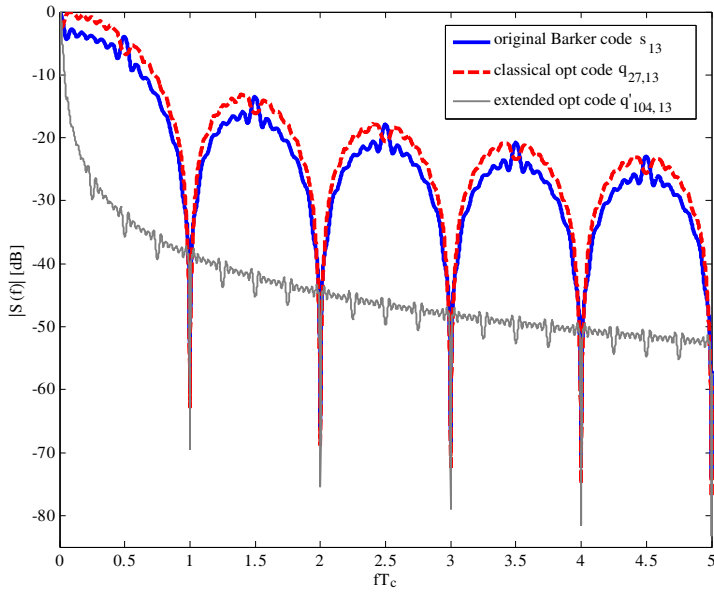
Figure 3. $S(f)$ magnitude corresponding to Barker case.
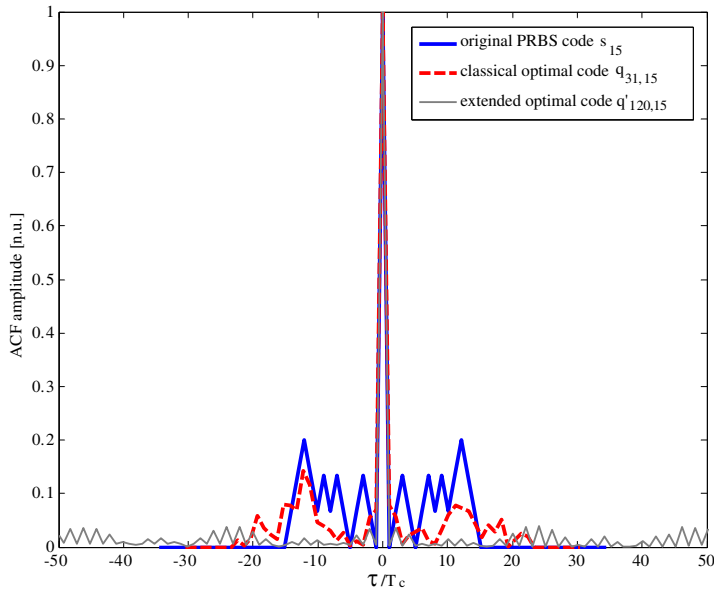
Figure 4. ACF corresponding to PRBS case.
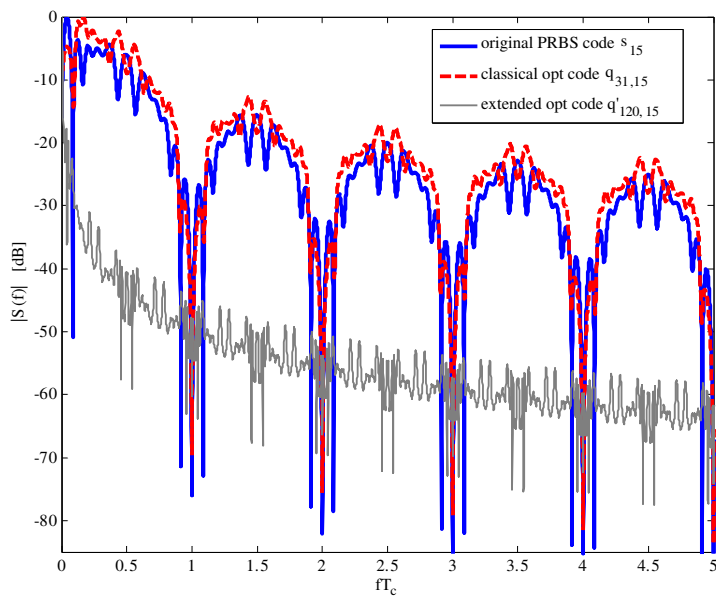
Figure 5. $S(f)$ magnitude corresponding to PRBS case.
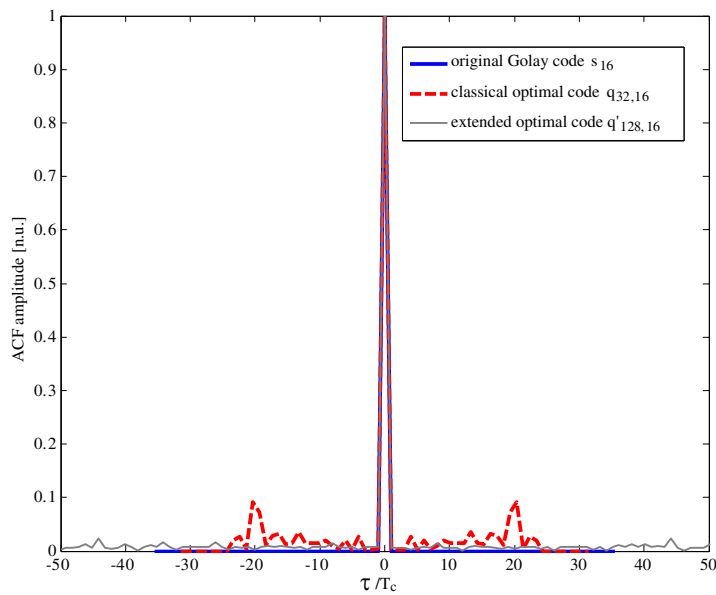
Figure 6. ACF corresponding to Golay case.
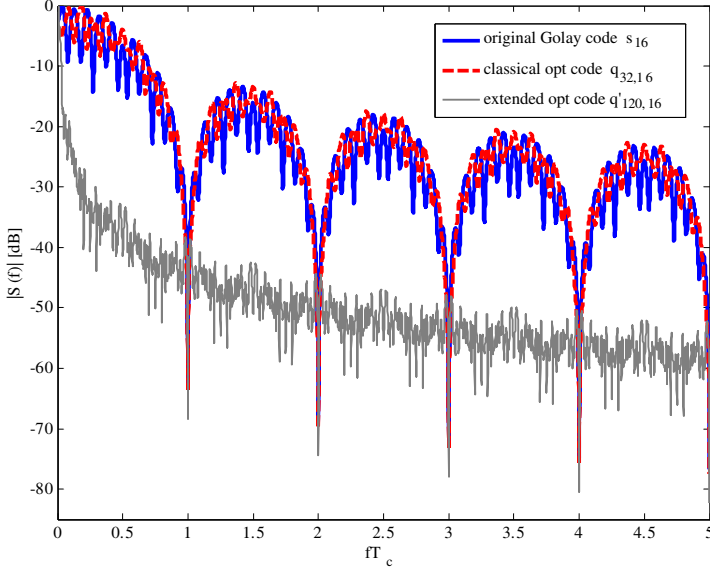
Figure 7. $S(f)$ magnitude corresponding to Golay case.

$1, 1, -1, 1$}. In Figs. 2–7, the third plot is related to the extended optimal filtering technique proposed in this paper, as detailed in Subsection 3.2. We should notice that $K = 2M$ for the Golay case since each original single sequence of the pair is even length, whereas $K = 2M + 1$ for the Barker and PRBS cases due to the odd length of these codes.

The classical optimal filtering technique [2, 3] is used to obtain the code $q = \{q_K\}$ by minimizing the energy E in (3) of the correlation between q and the original signal $s = \{s_M\}$ with $K \geq M$:

$$y = q^* \cdot \Lambda \tag{1}$$

$$\Lambda = \begin{bmatrix} s_K & \ldots & s_2 & s_1 & 0 & \ldots & 0 \\ 0 & s_K & \ldots & s_2 & s_1 & 0 & 0 \\ & & & \ldots & & & \\ 0 & \ldots & 0 & s_K & \ldots & s_2 & s_1 \end{bmatrix}_{Kx(2 \cdot K - 1)} \tag{2}$$

$$E = y \cdot y^H = q^* \cdot \left(\Lambda \cdot \Lambda^H \right) \cdot q^T = q^* \cdot A \cdot q^T \tag{3}$$

The solution vector q that minimizes the energy E must satisfy two constraints: the matrix $A_{K \times K} = \Lambda \cdot \Lambda^H$ cannot be singular, and the zero-delay peak should remain unaffected to avoid the CCF distortion. Therefore, (3) is solved subject to the constraint indicated in (4)

$$s \cdot q^H = s \cdot s^H, \tag{4}$$

resulting in the optimal code vector q_K in (5),

$$q_K = \frac{s \cdot A^{-1} \cdot \left(s \cdot s^H\right)}{s \cdot A^{-1} \cdot s^H}, \tag{5}$$

with length $K \geq M$. We can notice that the transformation by (5) turns the originally binary code s_M into a multilevel or m-ary code. More specifically, the final achieved code q results to be K-ary.

The reduction in the SLL is proportional to the length K; an obvious fact that larger codes yields lower SLL. As we illustrated in Figs. 2, 4 and 6, for this classical version of the optimal filtering technique, the CCF for the code q_K presents an unequal distribution of the SL energy. We discuss a possible solution to this problem in the following subsection.

2.2. Modification of Classical Optimal Filters

It may be noted in (5) that if $K > M$, then the original sequence $\{s = s_M\}$ with length M must be filled with $(K - M)$ zeros, such that the elements of s, $\{s_{M+1}, s_{M+2}, \ldots, s_K\} = 0$. If the null elements, $\{s_{M+1}, s_{M+2}, \ldots, s_K\}$ are placed as indicated above, it produces an asymmetrical CCF in terms of unequal distribution of the sidelobes, resulting in large sidelobes located close to the main peak. This would result in masking the weaker returns from a target located next to a stronger target or a stronger clutter. Therefore, we propose the distribution of the $(K - M)$ null elements in (6) so that symmetrical and spread-out sidelobe distribution of the resultant CCF is achieved. The original code s with length M turns into an intermediate code s' with length K, as indicated in (6):

$$s' = \left\{ \bar{\mathbf{O}}_{(K-M)/2} \quad s_M \quad \ldots \quad s_1 \quad \bar{\mathbf{O}}_{(K-M)/2} \right\}_K \tag{6}$$

where $\bar{\mathbf{O}}_{(K-M)/2}$ denotes a vector of $(K - M)/2$ null elements.

However, this code is not optimum in terms of simultaneous SLL and OBS capabilities, even when the length K is very large.

3. PROPOSED EXTENDED OPTIMAL FILTERING TECHNIQUE

The code q_K in (5) results in a symmetrical matrix if it is applied to codes s_M with some kind of symmetry or repetitive pattern, such as the Barker codes, as explained in Subsection 2.1 above. For a transmit sequence s_M with non-repetitive behaviour, such as PRBS, a redistribution of $(K - M)$ null elements as indicated in (6) must be adopted to achieve the symmetry. We propose a transformation of the

original code $\{s = s_M\}$, into a new intermediate code s'', $\{s''_{2M}\}$, as indicated in (7):

$$s'' = \{s_1 \quad -s_M \quad s_2 \quad -s_{M-1} \quad s_3 \quad -s_{M-2} \quad \ldots \quad s_M \quad -s_1\}_{2M} \quad (7)$$

A skew-symmetrical binary sequence s'' is achieved by the transformation proposed in (7). We also require a similar distribution of the $(K - 2M)$ null elements as in (6), so the final intermediate code s'' is given as in (8):

$$s'' = \{\bar{\boldsymbol{O}}_{(K-2M)/2} \ s_1 \ -s_M \ s_2 \ -s_{M-1} \ s_3 \ -s_{M-2} \ldots s_M \ -s_1 \ \bar{\boldsymbol{O}}_{(K-2M)/2}\}_{2M} \quad (8)$$

If we now apply the optimal filter process to this new code s'' (8), we obtain an extended code $q'_{K'}$ with a length $K' = 2 \cdot K \geq 2 \cdot M$ that follows the same expression given in (5), but with s'' (8) replacing s in (5). In the following subsections, we used this technique for three types of binary codes, namely PRBS, Golay, and Barker codes. We can notice that K' is an entire multiple of the original length M for the Barker, PRBS and Golay cases due to the even length of the corresponding intermediate sequence s''.

We also observe that the arrangement proposed in (8) maintains the skew-symmetry of the extended code. For this reason the CCF undergoes a remarkable improvement in terms of SSL and ISL, as demonstrated below.

3.1. Application of Extended Optimal Filters to Barker Codes

It may be observed in Fig. 2 and Fig. 3 that the improvement in terms of both ISL and OBS is also noteworthy when the proposed technique is used on the 13-bit Barker code s_{13} (given in Subsection 2.1), resulting in the extended code tagged $q'_{104,13}$ (given in Appendix A).

The ISL improvement Δ_{ISL}, the OBS improvement Δ_{OBS}, and the spectral decay can be shown to follow (9)–(11):

$$\Delta_{\mathrm{ISL}} = 10 \cdot \log_{10}\left(\frac{K'}{2M}\right) \quad [\mathrm{dB}] \quad (9)$$

$$\Delta_{\mathrm{OBS}} = 10 \cdot \log_{10}\left(\frac{K'^3}{4M^2}\right) \quad [\mathrm{dB}] \quad (10)$$

$$S(f)_{q'_{K',M'}} = 20 \cdot \log_{10}\left(\frac{10M}{K'^2} \cdot \frac{1}{f}\right) \quad [\mathrm{dB}] \quad (11)$$

The parameter Δ_{OBS} indicates the ratio between the levels of the first spectral sidelobe corresponding to codes s_M and $q'_{K',M}$, evaluated at $1.5/T_c$, T_c being the chip period.

3.2. Applications of Extended Optimal Filters to PRBS

We have used the extended optimal filtering in (7) with the same original PRBS code s_{15} given in Subsection 2.1, for $K' = 8 \cdot M$, $M = 15$, to produce the extended code $q'_{120,15}$ (given in Appendix B). The CCF and the $S(f)$ corresponding to the extended code $q'_{120,15}$ are shown in the third plot of Figs. 4 and 5. It may be noted in Fig. 4 that the proposed technique has resulted in a CCF with symmetrical pattern. We may also observe that the new code simultaneously optimizes both CCF SLL and frequency spectrum $S(f)$ corresponding to $q'_{120,15}$, thereby providing significant OBS. Furthermore, the improvement in the ISL reduction is equivalent to an extension of the original signal length s from M to $8M$.

Simulations have been performed for different values of M within the range $[15, 2^{13} - 1]$ and $K' = r \cdot 2 \cdot M$, $r = 1, 2, \ldots$. We noted that the ISL improvement Δ_{ISL} follows (12), while the OBS improvement Δ_{OBS} follows (13):

$$\Delta_{\text{ISL}} = \text{ISL}_s - \text{ISL}_{q'} = 10 \cdot \log_{10} \left(\frac{K'}{M} \right) \quad [\text{dB}] \quad (12)$$

$$\Delta_{\text{OBS}} = \text{OBS}_s - \text{OBS}_{q'} = 10 \cdot \log_{10} \left(\frac{K'^3}{2M^2} \right) \quad [\text{dB}] \quad (13)$$

The value Δ_{ISL} tends asymptotically to $-50\,\text{dB}$ after $K \geq 32M$. For $S(f)$, the Δ_{OBS} is about $35.5\,\text{dB}$ for $K' = 8 \cdot M$, ensuring a minimum OBS improvement of $25\,\text{dB}$ when compared to that of $K' = 2 \cdot M$. The $S(f)$ tail decay for the extended code $q'_{K',M}$ can be evaluated using (14):

$$S(f)_{q'_{K',M'}} = 20 \cdot \log_{10} \left(\frac{3M}{K'^2} \cdot \frac{1}{f} \right) \quad [\text{dB}] \quad (14)$$

The main advantage derived from the use of the extended optimal filter is that both ISL and OBS are reduced in direct proportion to the ratio K'/M without distorting the main CCF peak. The effect on both ISL and OBS is due to the time spreading effect of the optimal filters on the original signal. The extended code $q'_{K',M}$ has the same energy as in s'_{2M}, resulting in an unaltered main CCF peak as in (4), and distributing the SL energy by a time spreading factor K'/M.

From (9)–(11) we observe that Δ_{ISL} and Δ_{OBS} are lower than that of obtained for the PRBS case given in (12)–(13). However, the frequency spectral tail decay is steeper.

3.3. Applications of Extended Optimal Filters to Golay Code Pairs

For the Golay case, the ISL level, corresponding to a perfect code, is null. So, we can only band-limit its spectrum to comply with emission regulations or to decrease and/or eliminate the detection and intercept probability. The technique proposed for the *PRBS* case in Subsection 3.2 is also valid for Golay complementary code pairs. The expressions for Δ_{OBS} and the spectrum decay for the Golay single sequences can be shown to follow (15)–(16):

$$\Delta_{\text{OBS}} = 10 \cdot \log_{10}\left(\frac{K'^3}{8M^2}\right) \quad [\text{dB}] \tag{15}$$

$$S\left(f\right)_{q'_{K',M'}} = 20 \cdot \log_{10}\left(\frac{8M}{K'^2} \cdot \frac{1}{f}\right) \quad [\text{dB}] \tag{16}$$

The CCF and $S(f)$ corresponding to the Golay extended optimal filter are shown in Fig. 6 and Fig. 7, respectively. For these plots, we have used the same original Golay pair of codes sa_{16}, sb_{16} indicated in Subsection 2.1, to produce the extended code $q'_{128,16}$ (given in Appendix C).

3.4. Comparison of Extended Optimal Codes to Other Windowing Techniques

In Table 1, we compare the CCF main peak loss, the sidelobe reduction Δ_{ISL}, and the OBS, Δ_{OBS} achieved using classical windowing techniques, and the extended optimal filters presented in this paper. It may be observed that, in terms of OBS, the best performance corresponds to the Blackman window. However, the extended codes

Table 1. Comparison of various filtering and windowing techniques.

Sequence		PRBS (*M=15*) / Golay (*M=16*) / Barker (*M=13*)		
Parameter		ACF peak attenuation [dB]	*OBS* [dB]	*ISL* [dB]
Window type	Rectangular	0 / 0 / 0	-2.04	0 / 0 / 0
	Hamming	0.73 /1.36 / 0.73	25.5	-2.93 / 0 / 2.67
	Hanning	0.67 / 1.78 / 0.67	16.5	-2.76 / 0 / 2.46
	Blackman	0.57 / 2.39 / 0.57	41.5	-3.07 / 0 / 2.73
	Kaiser (β =2)	2.76 / 4.41 / 2.76	30.5	-2.97 / 0 / 2.67
Classical optimal $q_{K=8M+1,M}$		0 / 0 / 0	1 / 1 / -1	3.32 / -156.29 / 0.9
Extended optimal $q'_{K'=8M,M}$		0 / 0 / 0	35.5 / 30 / 37	9 / -154.23 / 6

proposed in this paper offer simultaneous improvement in Δ_{ISL} and Δ_{OBS} while retaining the main CCF peak unaltered.

4. DOPPLER AND MULTIPATH CAPABILITY OF EXTENDED OPTIMAL CODES

In Fig. 8, we show the AF magnitude $|\chi(\tau; \nu)|$ corresponding to the PRBS extended code $q'_{120,15}$. An accurate performance in both range and Doppler shift may be noted. The spreading of the SL energy by the spreading factor K'/M is the key for this improved performance.

Additionally, the multipath detection capability of the original signal s_M is not affected by its transformation into the extended code $q'_{K',M}$. In Fig. 9, we have depicted an example of multipath resolution corresponding to the extended code $q'_{120,15}$ obtained from the same original PRBS code s_{15} given in Subsection 2.1, for $K' = 8 \cdot M$, $M = 15$. Four multipath components were placed at delays $2 \cdot Tc, 4 \cdot Tc, 6 \cdot Tc$ and $8 \cdot Tc$, with amplitudes of $0.75\,\text{V}, 0.5\,\text{V}, 0.25\,\text{V}$ and $0.125\,\text{V}$ respectively. The result shows that the new code $q'_{K',M}$ offers a multipath detection as good as the original signal s_M, and this is even better in the case of low level amplitude echoes that can be undetected for the original signal due to the large intrinsic ISL value present in the PRBS.
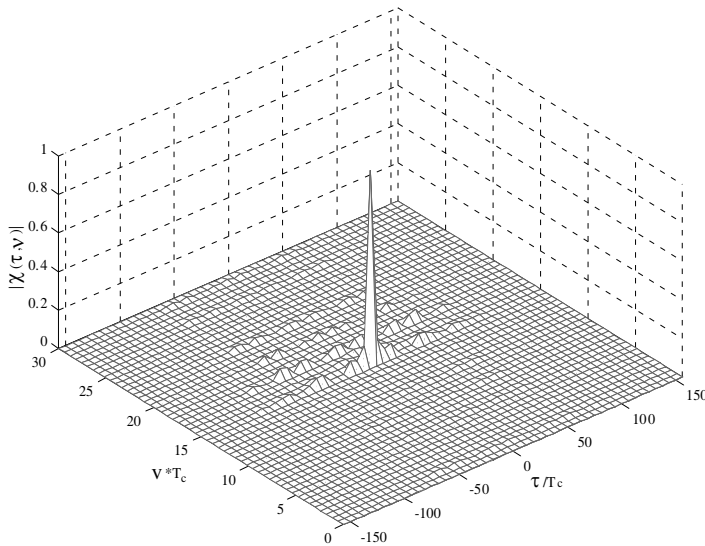
Figure 8. Normalized ambiguity function, $|\chi(\tau; \nu)|$ corresponding to PRBS $q'_{120,15}$, $K' = 8M$.
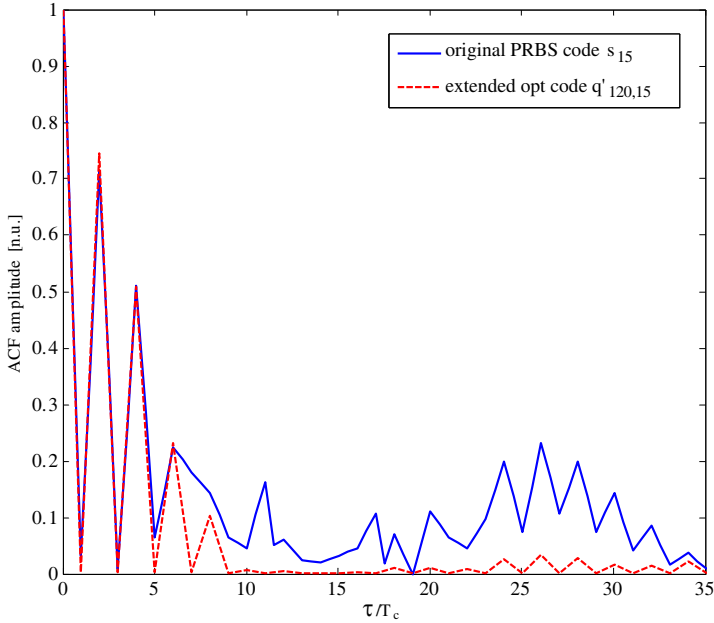
Figure 9. An example of the multipath resolution capability of the extended code $q'_{K',M}$, $K' = 8M = 120$.

5. SIMULATIONS RESULTS

Following we summarize the simulations done in previous sections. The original Barker sequence s_{13} with length $M = 13$ has derived in the optimal code $q_{27,13}$ (with length $K = 2 \cdot M + 1$) and $q'_{104,13}$ (with length $K' = 8 \cdot M$). In Appendix A, we detail the three codes, s_{13}, $q_{27,13}$ and $q'_{104,13}$. In a comparative way, the CCF's corresponding to these three codes have been shown in Fig. 2. The frequency spectra $S(f)$ of the three sequences are comparatively shown in Fig. 3.

In a similar way, for a PRBS code s_{15} with length $M = 15$, we have obtained the optimal code $q_{31,15}$ (with length $K = 2 \cdot M + 1$) and the extended code $q'_{120,15}$ (with length $K' = 8 \cdot M$), as indicated in Appendix B. The CCF's corresponding to the three sequences s_{13}, $q_{31,15}$ and $q'_{120,15}$ have been jointly plotted in Fig. 4, and their frequency spectra $S(f)$ are shown in Fig. 5.

In a similar way, for a pair of Golay codes s_a and s_b, each with length $M = 16$, we have obtained the optimal codes $qa_{32,16}$ and $qb_{32,16}$ (with length $K = 2 \cdot M$) and the extended codes $qa'_{128,16}$ and $qb'_{128,16}$ (with length $K' = 8 \cdot M$). The codes derivation can be followed in

Appendix C. The corresponding CCF's and $S(f)$ are shown in Fig. 6 and Fig. 7, respectively.

Finally, we have also simulated the performance of the presented approach in terms of multipath and Doppler resolution, just for the case of PRBS extended code $q'_{120,15}$ (with length $K' = 8 \cdot M$), as per Fig. 8 and Fig. 9, respectively.

6. APPLICABILITY

In radar applications, appropriate transmit waveforms are of vital importance for applications such as target detection, non-ambiguous estimation of range and range-rate, accuracy, resolution, and clutter rejection. Therefore, the radar designer has to carefully examine and choose the transmit waveforms to achieve the desired objectives of the intended system. In general, the optimal design, involving both hardware and software components, usually performs optimally under specific operational conditions for which the system was designed. The performance of such a system may degrade if the operational environment undergoes an adverse change. Examples of such environmental degradation could include, among others, the increasing noise level, the changing propagation channel, jamming or interference(s), the nature of the targets, and so on. The radar system should, therefore, be capable of dynamically adjusting system parameters to optimize its performance. Adaptive techniques such as antenna beamforming or space-time adaptive processing [9, 10], mainly at the receiver end, have been tried to mitigate these effects.

At the transmitter end, the adaptive-on-transmit (AT) methodologies based on the waveform design constitute the biggest family of AT approaches. The concept of AT is not new, having been considered at various stages in the past [11–17]. Technological advances over the last couple of decades in generating and manipulating digital waveforms have provided further impetus to real-time AT waveforms. AT methodologies can be further subdivided into waveform selection and waveform design. In the first case, the parameters of the transmitted signal can be adaptively selected from a predefined set. In the second case, the parameters are dynamically estimated according to the changing operational environment, thereby demanding large computational power. Both AT techniques, selection or design, are further constrained by the system hardware limitations. The trade-off between the system capabilities and the waveform-based AT approach makes it much harder to design an optimal performing system under all operational conditions.

Waveform-filter pair [18] is another AT technique used to overcome

the constraint imposed upon the waveform selection and/or design technique. This technique has an additional advantage in terms of the sidelobe reduction in the CCF for systems utilizing noise-like or pseudo-noise binary sequences, such as Barker codes, Minimum Peak Sidelobe (MPS) codes, and PRBS (also called maximal length sequences or m-sequences). PRBS waveforms are preferred for advantages over other binary codes and deterministic waveforms. These include low probability of detection (LPD) and intercept (LPI), better immunity to external electromagnetic interference (EMI), improved spectral efficiency, and immunity to jamming.

However, the use of PRBS, gives rise to high correlation SLL, also called code self noise [19]. This latter is a well known problem in radar and communication systems that use binary sequences [20]. The longest known Barker code is a length 13 code with corresponding peak sidelobe ratio (PSL) of $-22.3\,\mathrm{dB}$ [3, 21]. One of the best known MPS codes is of length 105 with corresponding PSL of $-26.44\,\mathrm{dB}$ [3, 21]. PRBS provide a PSL that approach $10 \cdot \log_{10}(1/M)$, M being the code length [21]. The code self-noise makes it harder to detect the weaker echoes from smaller targets, thereby limiting the dynamic range of the radar system utilizing such waveforms. Different techniques have been proposed to minimize the SLL; these include windowing [22, 23], coding [24–27], mismatched filtering [28–34], and others [35, 36], including waveform design [37–42]. In this latter group, we can include the Golay code pairs with null levels of SSL and ISL; however, despite of the advantages provided by the use of these code pairs, its use requires the transmission and reception of two single sequences instead of one [40] slowing down the response time of the systems.

Overall system performance can attain real-time enhanced detection performance by dynamically adapting the parameters of the transmitted waveforms such that SLL reduction is achieved. Adaptive sidelobe mitigation technique is however linked to the length M of the sequence. Although, varying the sequence length M to reduce the SLL can be seen as an effective AT technique, subject to hardware constraints, it usually works in trade-off with the spectral purity of the transmitted waveform. In general, binary sequences have significant out-of-band spectral leakage and are not spectrally clean or fully band-limited. Spectrally clean transmitted waveform is an important design issue, if emission control levels must be respected. It also influences other system operational features, such as LPD and LPI.

Theoretically, the extended optimal filtering technique herein proposed can provide simultaneously both lower aperiodic CCF sidelobe levels and spectrally clean waveforms. The main CCF peak remains unaffected, resulting in a larger dynamic range of the system

and better ability to detect weaker returns. The proposed technique has also shown to be Doppler resistant, and with a reliable multipath capability.

It can be used in real-time adaptive-on-transmit systems to mitigate the sidelobe noise due to the dynamically changing operational environment. It would only require to enlarge the code length K' to achieve the desired specifications. So, at the receiver end, even in presence of adverse conditions, the received signal enables an optimum information retrieval. Despite of the longer time needed to transmit the resulting code, this fact does not necessarily lead to require generating or receiving hardware which additional improved specifications other than a larger memory buffer with is a not significant feature in the hardware existing at present. However, the additional transmitting time required could lead to larger system overhead which can affect the overall system performance in such a way that must be evaluated from the point of view of the specific advantage provided by the new code, such as the OBS or SSL improvement.

Extended codes, as herein proposed, possess narrowband features in its frequency spectrum. The no-lobule shape frequency spectrum $S(f)$ achieved by the extended codes impacts positively other features such as the low probability of detection (LPD) and intercept (LPI), better immunity to external electromagnetic interference (EMI), improved spectral efficiency, and immunity to jamming. The like-narrowband property would allow its use in spectrum sharing applications. In this scenario the extended codes can help to reduce the mutual interference between users.

Due to the above features, they could be applicable in communications with large number of interferers and jammers, either natural or man-made, for both military and non-military applications. For instance, it would be possible to deploy a communication system in any portion of the spectrum due to the small frequency bandwidth required, thereby avoiding interference with pre-existing systems (multifrequency allocation). The extended codes could significantly improve the safety level of critical communications.

Furthermore, the ability to use the extended codes with minimum SL would greatly enhance the radar image quality within a given medium, especially in ultrawideband (UWB) systems.

7. CONCLUSIONS

A design method to obtain extended optimal codes with optimal performance in terms of CCF SLL, ISL and OBS is proposed. The method is derived from the classical optimal filtering technique. It

requires two steps to modify the input signal in order to achieve an optimal output waveform in both CCF and frequency spectrum. The first arrangement only achieves an improvement in terms of equal distribution and amplitude level of the CCF sidelobes, i.e., CCF SSL and CCF ISL. In the second step, named extended codes, we propose to provide skew-symmetry to the original input binary code as a modification suitable to achieve a simultaneous improvement in terms of equal distribution of the CCF secondary sidelobes and OBS.

The extended codes proposed in this paper offer simultaneous improvement in Δ_{ISL} and Δ_{OBS}, while retaining the main CCF peak unaltered. Such extended codes can be applied to any symmetric (such as Barker) or non-symmetric codes, such as PRBS and Golay complementary codes. These codes would be suitable for AT system to respond to the changing operational environment by extending the length K' of the code. The parameter K' has been found to be closely related to the value of both CCF sidelobes and out-of-band spectral purity. This latter feature is of importance in scenarios necessitating strict OBS requirements. The proposed technique has also been shown to have accurate range-Doppler and multipath capabilities. The like-narrowband shape of the frequency spectrum $S(f)$ related to the proposed extended codes impacts positively such important features as multiuser interference, and broadens the application field. This property would also contribute to reduce the interference with existing systems on a given frequency band of interest, providing so an interesting multi-frequency allocation feature.

ACKNOWLEDGMENT

APPENDIX A.

We provide here the original Barker sequence s_{13} with length $M = 13$, the intermediate code s_{27} with the $(K - M)$ null elements, and the final optimal code $q_{104,13}$ as per Subsection 3.1 with length $K = 2M + 1$:

$$s_{13} = \{-1, -1, -1, -1, -1, 1, 1, -1, -1, 1, -1, 1, -1\}.$$
$$s_{27} = \{-1, -1, -1, -1, -1, 1, 1, -1, -1, 1, -1, 1, -1, 0, 0, 0, 0, 0, 0, 0,$$
$$0, 0, 0, 0, 0, 0, 0\}.$$

$$q_{27,13} = \{-0.7979, -1.1068, -0.8133, -1.1016, -0.8232, 1.1079,$$
$$1.3694, -1.0835, -0.8408, 1.1258, -0.8486, 1.1307, -0.8505,$$
$$0.0294, 0.1854, -0.0628, 0.1176, -0.1546, 0.049, -0.0623,$$
$$0.1631, -0.1525, 0.0931, -0.0587, 0.0224, 0.0355, -0.0485\}.$$

Following, we show the modification of the classical optimal code by redistributing the $(K\text{-}M)$ zeros as indicated in (6), achieving a code $q_{K,M}$ with the same length $K = 2M + 1$ corresponding to the same original Barker sequence s_{13}:

$$s'_{27} = \{0, 0, 0, 0, 0, 0, 0, -1, -1, -1, -1, -1, 1, 1, -1, -1, 1, -1, 1, -1,$$
$$0, 0, 0, 0, 0, 0, 0\}.$$

$$q_{27,13} = \{-0.072, 0.0642, -0.1628, 0.1351, -0.0699,$$
$$0.2049, 0.0234, -0.8214, 1.1201, -0.8385, 1.1143, -0.8497,$$
$$-1.0888, 1.3344, 1.0888, -0.8497, -1.1143, -0.8385,$$
$$-1.1201, -0.8214, -0.0234, 0.2049, 0.0699, 0.1351, 0.1628,$$
$$0.0642, 0.072\}.$$

Extended optimal code with length $K' = 8M$ and intermediate code s''_{104} corresponding to an original Barker sequence with length $M = 13$:

$$s''_{104} = \{0, 0, 0, 0, 0, 0, 0, 0, 0, 0, 0, 0, 0, 0, 0, 0, 0, 0, 0, 0, 0, 0, 0, 0, 0, 0,$$
$$0, 0, 0, 0, 0, 0, 0, 0, 0, 0, 0, -1, 1, -1, -1, -1, 1, -1, -1, -1,$$
$$1, 1, 1, 1, -1, -1, -1, -1, 1, 1, 1, -1, 1, 1, 1, -1, 1, 0, 0, 0, 0,$$
$$0, 0, 0, 0, 0, 0, 0, 0, 0, 0, 0, 0, 0, 0, 0, 0, 0, 0, 0, 0, 0, 0, 0, 0,$$
$$0, 0, 0, 0, 0, 0, 0\}.$$

$$q'_{104,13} = \{-0.036, -0.1016, -0.1367, -0.2022, -0.2257, -0.2876,$$
$$-0.2929, -0.3548, -0.3541, -0.4122, -0.4036, -0.4617,$$
$$-0.4254, -0.4796, -0.4733, -0.5276, -0.6267, -0.6771,$$
$$-0.8561, -0.9065, -1.1434, -1.1898, -1.5524, -1.5988,$$
$$-1.9739, -2.0164, -2.1937, -2.2362, -2.3864, -2.4304,$$
$$-2.7881, -2.832, -3.1224, -3.1676, -3.3342, -3.3794,$$
$$-3.8074, -3.8536, -3.8263, -3.8725, -2.2466, -2.2934,$$
$$-0.0693, -0.1161, 1.5372, 1.4899, 3.6928, 3.6455,$$
$$5.3033, 5.2558, 3.0332, 2.9858, 0.252, 0.2045, 2.3322, 2.2848,$$
$$3.9425, 3.8953, 1.5979, 1.5506, 3.2039, 3.1571, 0.8393,$$
$$0.7925, 2.4184, 2.3722, 2.2527, 2.2066, 1.7785, 1.7333,$$
$$1.8095, 1.7643, 1.474, 1.43, 1.6996, 1.6556, 1.5054, 1.4629,$$

$$1.5554, 1.5129, 1.1378, 1.0914, 1.3611, 1.3147, 1.0778,$$
$$1.0274, 1.1057, 1.0554, 0.9562, 0.902, 0.7871, 0.7328, 0.7692,$$
$$0.7111, 0.5863, 0.5282, 0.5289, 0.467, 0.3485, 0.2866, 0.2631,$$
$$0.1976, 0.1016, 0.036\}.$$

APPENDIX B.

We provide here the original PRBS sequence s_{15} with length $M = 15$, the intermediate code s''_{120} and the final extended optimal code $q'_{120,15}$ as per Subsection 3.2:

$s_{15} = \{-1, -1, -1, 1, -1, -1, 1, 1, -1, 1, -1, 1, 1, 1, 1\}.$

$s''_{120} = \{0, 0, 0, 0, 0, 0, 0, 0, 0, 0, 0, 0, 0, 0, 0, 0, 0, 0, 0, 0, 0, 0, 0, 0, 0, 0, 0, 0, 0, 0,$
$\qquad 0, 0, 0, 0, 0, 0, 0, 0, 0, 0, 0, 0, 0, 0, 0, 0, 0, 0, 0, -1, -1, -1, -1, -1,$
$\qquad -1, 1, -1, -1, 1, -1, -1, 1, 1, 1, -1, -1, -1, 1, 1, -1, 1, 1, -1,$
$\qquad 1, 1, 1, 1, 1, 1, 0, 0, 0, 0, 0, 0, 0, 0, 0, 0, 0, 0, 0, 0, 0, 0, 0, 0, 0, 0,$
$\qquad 0, 0, 0, 0, 0, 0, 0, 0, 0, 0, 0, 0, 0, 0, 0, 0, 0, 0, 0, 0, 0, 0, 0, 0\}.$

$q'_{120,15} = \{0.2432, 0.3157, 0.6606, 0.7388, 1.209, 1.5008, 1.5672, 1.1303,$
$\qquad 1.6674, 1.7232, 1.6562, 1.7081, 1.5192, 1.5629, 1.3528, 1.4068,$
$\qquad 1.1764, 1.2257, 1.1076, 1.1696, 1.3113, 1.3808, 1.8721, 1.9566,$
$\qquad 2.5712, 2.6754, 3.2015, 3.3138, 3.9284, 4.0427, 4.6366, 4.735,$
$\qquad 4.7691, 4.8566, 4.3393, 4.4152, 3.9287, 4.0031, 3.7252, 3.805,$
$\qquad 3.6443, 3.7321, 3.663, 3.7636, 3.6009, 3.7107, 4.6850, 4.8051,$
$\qquad 6.9989, 7.1235, 7.7206, 7.8451, 6.3859, 6.5034, 8.2403, 8.3452,$
$\qquad 10.2166, 0.3091, 7.9548, 8.0390, 4.8865, 4.9707, 7.4044, 7.4969,$
$\qquad 6.0033, 6.1082, 9.3527, 9.4702, 7.7408, 7.8653, 5.8293, 5.9539,$
$\qquad 3.5925, 3.7126, 1.3510, 1.4608, 2.6336, 2.7342, 2.4817, 2.5696,$
$\qquad 4.1858, 4.2656, 3.3185, 3.3929, 3.1594, 3.2354, 2.9006, 2.9881,$
$\qquad 2.8108, 2.9091, 3.5699, 3.6841, 2.7199, 2.8322, 2.3232, 2.4274,$
$\qquad 0.7705, 0.8551, 0.3039, 0.3733, 0.2204, 0.2825, 0.5756, 0.6249,$
$\qquad 1.2437, 1.2977, 1.1430, 1.1868, 1.2848, 1.3367, 0.9138, 0.9696,$
$\qquad 0.9669, 1.0333, 0.8709, 0.9495, 0.6953, 0.7736, 0.4435, 0.516\}.$

APPENDIX C.

For the first item of the pair, we provide here the original Golay single code with length $M = 16sa_{16}$, the intermediate code sa''_{128} and the

final extended optimal code $qa'_{128,16}$ as per Subsection 3.3:

$sa_{16} = \{1,1,1,-1,1,1,-1,1,1,1,1,-1,-1,-1,1,-1\}.$

$sa''_{128} = \{0,0,0,0,0,0,0,0,0,0,0,0,0,0,0,0,0,0,0,0,0,0,0,0,0,0,0,$
$\qquad 0,0,0,0,0,0,0,0,0,0,0,0,0,0,0,0,0,0,0,0,0,0,1,1,1,-1,$
$\qquad 1,1,-1,1,1,1,1,-1,-1,-1,1,-1,1,-1,1,1,1,1,-1,-1,$
$\qquad -1,-1,1,-1,-1,1,-1,-1,-1,-1,0,0,0,0,0,0,0,0,0,0,0,$
$\qquad 0,0,0,0,0,0,0,0,0,0,0,0,0,0,0,0,0,0,0,0,0,0,0,0,0,0,$
$\qquad 0,0,0,0,0,0,0,0,0,0\}.$

$qa'_{128,16} = \{0.0715, 0.1122, 0.1784, 0.6056, 0.6705, 0.5371, 0.5957, 0.4116,$
$\qquad 0.4732, 0.5645, 0.6197, 0.9807, 1.0346, 0.9254, 0.9746, 0.4663,$
$\qquad 0.5172, 1.0429, 1.0766, 1.3601, 1.3941, 0.5612, 0.6243, 0.8288,$
$\qquad 0.8915, 1.5213, 1.5874, 1.2947, 1.3567, 0.9278, 0.9988, 0.844,$
$\qquad 0.9105, 1.92, 1.9852, 1.4400, 1.5031, 0.1419, 0.2087, 1.6725,$
$\qquad 1.7234, 1.7163, 1.7679, 0.0875, 0.1473, 0.6172, 0.6817, 0.9326,$
$\qquad 0.9959, 0.8650, 0.9263, -0.4344, -0.3665, -1.4354, -1.3691,$
$\qquad 0.8729, 0.9367, -1.3102, -1.2461, -3.4701, -3.4018,$
$\qquad -0.3895, -0.3314, -2.3134, -2.2561, -5.4731, -5.415,$
$\qquad -7.2884, -7.2201, -9.4046, -9.3406, -6.0982, -6.0344,$
$\qquad -4.7647, -4.6984, -1.7089, -1.6411, -3.0981,$
$\qquad -3.0367, -1.5378, -1.4745, -2.1241, -2.0596, -0.0782,$
$\qquad -0.0183, -0.8927, -0.8411, -1.3796, -1.3287, -3.313,$
$\qquad -3.2461, -4.0801, -4.0171, -3.8085, -3.7432, -3.2350,$
$\qquad -3.1685, -2.2291, -2.1581, -2.5700, -2.5080, -1.7116,$
$\qquad -1.6454, -1.6933, -1.6307, -0.2715, -0.2084, -0.4355,$
$\qquad -0.4015, -0.1429, -0.1092, -1.0271, -0.9763,$
$\qquad -1.0910, -1.0418, -1.4362, -1.3823, -1.1067, -1.0515,$
$\qquad -1.0733, -1.0117, -1.0295, -0.9709, -0.8752, -0.8103,$
$\qquad -0.6686, -0.6024, -0.0715\}.$

And, for the second item of the pair, we provide the original Golay single code with length $M = 16sb_{16}$, the intermediate code sb''_{128} and the final extended optimal code $qb'_{128,16}$ as per Subsection 3.3:

$sb_{16} = \{1,1,1,-1,1,1,-1,1,-1,-1,-1,1,1,1,-1,1\}.$

$$sb''_{128} = \{0,0,0,0,0,0,0,0,0,0,0,0,0,0,0,0,0,0,0,0,0,0,0,0,0,0,0,$$
$$0,0,0,0,0,0,0,0,0,0,0,0,0,0,0,0,0,0,0,0,0,0,0,0,1,-1,1,1,$$
$$1,-1,-1,-1,1,-1,1,1,-1,1,1,1,-1,-1,-1,1,-1,-1,$$
$$1,-1,1,1,1,-1,-1,-1,1,-1,0,0,0,0,0,0,0,0,0,0,0,0,$$
$$0,0,0,0,0,0,0,0,0,0,0,0,0,0,0,0,0,0,0,0,0,0,0,0,0,0,$$
$$0,0,0,0,0,0,0,0,0\}.$$

$$qb'_{128,16} = \{\ 0.0602, -0.3375, -0.2721, -0.131, -0.0665, -0.0348,$$
$$0.0331, 0.0241, 0.094, 0.2475, 0.3232, 0.6192, 0.6939, 1.2154,$$
$$1.2931, 1.2046, 1.2814, 2.3255, 2.4165, 2.7328, 2.8248,$$
$$3.1772, 3.2444, 4.6029, 4.6669, 4.8402, 4.9003, 5.6935,$$
$$5.7535, 6.2874, 6.3403, 7.2595, 7.3076, 6.9127, 6.9603,$$
$$7.1529, 7.2004, 8.1487, 8.1975, 6.1985, 6.2345, 6.8583,$$
$$6.8929, 6.0038, 6.0463, 4.1784, 4.2247, 3.5601, 3.6074,$$
$$2.2164, 2.2612, 0.7904, 0.8413, -2.0235, -1.9695, -0.7076,$$
$$-0.6502, -3.7695, -3.7145, -5.9101, -5.8560, -3.8639,$$
$$-3.8022, -7.008, -6.944, -4.8452, -4.7835, -1.7892,$$
$$-1.7351, 0.6053, 0.6604, -1.5896, -1.5322, -3.6514,$$
$$-3.5974, -4.6819, -4.631, -3.1661, -3.1212, -3.2674,$$
$$-3.2202, -3.3602, -3.3138, -2.8626, -2.8201, -1.0557,$$
$$-1.0211, -1.0429, -1.007, -2.3534, -2.3046, -3.6798,$$
$$-3.6324, -2.9753, -2.9278, -1.9377, -1.8896, -1.611,$$
$$-1.5582, -1.9885, -1.9284, -1.5103, -1.4502, -0.8197,$$
$$-0.7557, -0.8296, -0.7624, -1.5362, -1.4442, -1.6027,$$
$$-1.5116, -0.9606, -0.8838, -0.2491, -0.1714, -0.2594,$$
$$-0.1847, -0.4145, -0.3388, -0.2393, -0.1694, 0.1409,$$
$$0.2089, 0.0756, 0.1401, -0.1551, -0.0896, -0.0602\}.$$

REFERENCES

1. Nunn, C. J. and G. E. Coxson, "Best-known autocorrelation peak sidelobe levels for binary codes of length 71 to 105," *IEEE Transactions on Aerospace and Electronic Systems*, Vol. 44, No. 1, 392–395, 2008.

2. Griep, K. R., J. A. Ritcey, and J. J. Burlingame, "Polyphase codes and optimal filters for multiple user ranging," *IEEE Transactions on Aerospace and Electronic Systems*, Vol. 31, No. 2, 752–767, April 1995.

3. Levanon, N. and E. Mozeson, *Radar Signals*, John Wiley & Sons, USA, 2000.

4. Chen, C.-Y., C.-H. Wang, and C.-C. Chao, "Complete complementary codes and generalized Reed-Muller codes," *IEEE Communications Letters*, Vol. 12, No. 11, 849–851, November 2008.

5. Golay, M. J. E. and D. J. Harris, "A new search for skew symmetric binary sequences with optimal merit factors," *IEEE Transactions on Information Theory*, Vol. 36, No. 5, 1163–1166, September 1990.

6. Golay, M. J. E., "The merit factor of long low autocorrelation binary sequences with optimal merit factors," *IEEE Transactions on Information Theory*, Vol. 28, 543–549, 1982.

7. Helleseth, T., D. Sarwate, H.-Y. Song, and K. Yang, *Third International Conference on Sequences and Their Applications–SETA*, revised selected papers, Seoul, Korea, October 24–28, 2004.

8. *Lecture Notes in Computer Science*, Vol. 3486, Tod Helleseth Ed., Springer, 2005.

9. Guerci, J. R. and S. U. Pillai, "Theory and application of optimum transmit-receive radar," *IEEE International Radar Conference*, 705–709, 2000.

10. Van Trees, H. L., *Optimum Array Processing*, Wiley Interscience, New York, 2002, ISBN 0471093904.

11. Van Trees, H. L., "Optimum signal design and processing for reverberation-limited environments," *IEEE Transactions on Military Electronics*, Vol. 9, No. 3, 212–229, 1965.

12. Athans, M. and F. C. Schweppe, "Optimal waveform design via control theoretic principles," *Information Control*, Vol. 10, 335–377, 1967.

13. DeLong, D. and E. Hofstetter, "On the design of optimum radar waveforms for clutter rejection," *IEEE Transactions on Information Theory*, Vol. 13, No. 3, 454–463, 1967.

14. Kincaid, T. G., "Optimum waveforms for correlation detection in the sonar environment noise-limited conditions," *The Journal of the Acoustical Society of America*, Vol. 44, No. 3, 787–796, 1968.

15. Gjessing, D. T., *Target Adaptive Matched Illumination Radar: Principles and Application*, Peter Peregrinus Ltd., 1986, ISBN: 0-86341-057-X.

16. Schreiber, H. H. and M. G. O'Connor, "Adaptive waveform radar," United States Patent 4,901,082, February 1990.

17. Bell, M. R., "Information theory and radar waveform design,"

IEEE Transaction on Information Theory, Vol. 39, No. 5, 1578–1597, September 1993.

18. Lee, S. P. and J. L. Uhran, "Optimum signal and filter design in underwater acoustic echo ranging systems," *IEEE Transactions on Aerospace and Electronic Systems*, Vol. 9, No. 5, 701–713, September 1973.

19. Kayani, J. K., "Development and application of spread spectrum ultrasonic evaluation technique," Ph.D. Dissertation, Iowa State University, Ames, IA, 1996.

20. Narayanan, R. M., X. Xu, and J. A. Henning, "Radar penetration imaging using ultra-wideband (UWB) random noise waveforms," *IEE Proc. on Radar, Sonar and Navigation*, Vol. 151, No. 3, 143–148, June 2004.

21. Richards, M. A., et al., *Principles of Modern Radar: Basic Principles*, Scitech Publishing, Inc., 2010.

22. Lewis, B. L. and F. F. Kretschmer, Jr., "A new class of polyphase pulse compression codes and techniques," *IEEE Transactions on Aerospace and Electronics Systems*, Vol. 17, No. 3, May 1981.

23. Lewis, B. L. and F. F. Kretschmer, Jr., "Linear frequency modulation derived polyphase pulse compression codes and techniques," *IEEE Transactions on Aerospace and Electronics Systems*, Vol. 18, No. 5, May 1981.

24. Lee, W. K., H. D. Griffiths, and L. Vinagre, "Developments in radar waveform design," *12th International Conference on Microwaves and Radar (MIKON)*, Vol. 4, 56–76, May 1998.

25. Lee, W. K., H. D. Griffiths, and R. Benjamin, "Integrated sidelobe energy reduction technique using optimal polyphase codes," *Electronics Letters*, Vol. 35, No. 24, November 1999.

26. Nunn, C. J. and G. E. Coxson, "Polyphase pulse compression codes with optimal peak and integrated sidelobes," *IEEE Transactions on Aerospace and Electronic Systems*, Vol. 45, No. 2, 775–781, April 2009.

27. Nunn, C. and G. Coxson, "Best known autocorrelation peak sideobe levels for binary codes of length 71 to 105," *IEEE Transactions on Aerospace and Electronic Systems*, Vol. 44, No. 1, 392–395, January 2008.

28. Ackroyd, M. H. and Ghani, "Optimum mismatched filters for sidelobe suppression," *IEEE Transactions on Aerospace and Electronic Systems*, Vol. 9, No. 2, 214–218, March 1973.

29. Molina, A. and P. C. Fannin, "Application of mismatched filter theory to bandpass impulse response measurements," *Electronics*

Letters, Vol. 29, No. 2, 162–163, January 1993.

30. Levanon, N., "Cross-correlation of long binary signals with longer mismatched filters," *IEE Proc. Radar, Sonar and Navigation*, 1–6, 2005.

31. Levanon, N. and A. Scharf, "Range sidelobes blanking by comparing outputs of contrasting mismatched filters," *IET Radar Sonar Navig.*, Vol. 3, No. 3, 265–277, 2009.

32. Levanon, N., "Noncoherent radar pulse compression based on complementary sequences," *IEEE Trans. on Aerospace and Electronic Systems*, Vol. 45, No. 2, 742–747, April 2009.

33. Bhatt, T. D., E. G. Rajan, and P. V. D. S. Rao, "Design of frequency-coded waveforms for target detection," *IET Radar Sonar Navig.*, Vol. 2, No. 5, 388–394, 2008.

34. Shinriki, M., H. Takase, and H. Susaki, "Periodic binary codes with zero and small time sidelobe levels," *IEE Proc. — Radar Sonar Navig.*, Vol. 153, No. 6, December 2006.

35. Lee, W.-K., "A pair of asymmetric weighting receivers and polyphase codes for efficient aperiodic correlations," *IEEE Communications Letters*, Vol. 10, No. 5, 387–389, May 2006.

36. Sebt, M. A., A. Sheikhi, and M. M. Nayebi, "Orthogonal frequency-division multiplexing radar signal design with optimized ambiguity function and low peak-to-average power ratio," *IET Radar Sonar Navig.*, Vol. 3, No. 2, 122–132, 2009.

37. Liu, B., "Orthogonal discrete frequency-coding waveform set design with minimized autocorrelation sidelobes," *IEEE Transactions on Aerospace and Electronic Systems*, Vol. 45, No. 4, 1650–1657, October 2009.

38. Searle, S. J., S. D. Howard, and W. Moran, "Formation of ambiguity functions with frequency-separated Golay coded pulses," *IEEE Transactions on Aerospace and Electronic Systems*, Vol. 45, No. 4, 1580–1597, October 2009.

39. Liu, J. and W. Chu, "Design of binary multiple level sequences," *IEEE Transactions on Aerospace and Electronic Systems*, Vol. 47, No. 1, 26–36, January 2011.

40. Alejos, A. V., M. G. Sánchez, and I. Cuiñas, "Improvement of wideband radio channel swept time cross-correlation sounders by using golay sequences," *IEEE Transactions on Vehicular Technology*, Vol. 56, No. 1, January 2007.

41. Zakeri, B. G., M. Zahabi, and S. Alighale, "Sidelobes level improvement by using a new scheme used in microwave pulse compression radars," *Progress In Electromagnetics Research*

Letters, Vol. 30, 81–90, 2012.

42. Lee, H. and Y.-H. Kim, "Weather radar network with pulse compression of arbitrary nonlinear waveforms: Ka-band test-bed and initial observations," *Progress In Electromagnetics Research B*, Vol. 25, 75–92, 2010.